International Journal of Pharmaceutics 391 (2010) 197–202

Contents lists available at ScienceDirect

International Journal of Pharmaceutics

journal homepage: www.elsevier.com/locate/ijpharm

Crystallographic, thermal and spectroscopic characterization of a ciprofloxacin saccharinate polymorph

C.B. Romañuk[a], Y. Garro Linck[b], A.K. Chattah[b], G.A. Monti[b], S.L. Cuffini[c], M.T. Garland[d], R. Baggio[e], R.H. Manzo[a], M.E. Olivera[a,*]

[a] Departamento de Farmacia, Facultad de Ciencias Químicas, Universidad Nacional de Córdoba, Ciudad Universitaria, 5016 Córdoba, Argentina and CONICET
[b] Facultad de Matemática, Astronomía y Física and IFFAMAF (CONICET), Universidad Nacional de Córdoba, 5016 Córdoba, Argentina
[c] Subsecretaria Ceprocor, Ministerio de Ciencias y Tecnología de la Provincia de Córdoba, Argentina and CONICET
[d] Departamento de Física, Facultad de Ciencias Físicas y Matemáticas and CIMAT, Universidad de Chile, Chile
[e] Departamento de Física, Comisión Nacional de Energía Atómica (CNEA), Buenos Aires, Argentina

ARTICLE INFO

Article history:
Received 26 November 2009
Received in revised form 17 February 2010
Accepted 1 March 2010
Available online 7 March 2010

Keywords:
Fluoroquinolone
Salts
Polymorphism
Solid-state characterization

ABSTRACT

A new polymorphic form of ciprofloxacin saccharinate (CIP-SAC II) is presented, and compared with CIP-SAC I, a different polymorph which we had previously reported. The characterization techniques used were single crystal and powder X-ray diffraction, differential scanning calorimetry, thermogravimetry analysis and infrared and ^{13}C solid-state nuclear magnetic resonance spectroscopy. The results obtained from these techniques are consistent. Differential scanning calorimetry and thermogravimetric analysis showed that the reaction between the precursors is completed and the crystalline forms of both salts obtained (I and II) are highly pure. Infrared spectroscopy gave clear evidence of a salt formation. Solid-state nuclear magnetic resonance spectroscopy would indicate some degree of qualitative similarity in the intermolecular interaction scheme in both polymorphs, while thermal analysis data might indicate a difference in quantitative terms. A thorough single crystal structure determination of the new form CIP-SAC II allowed disclosing the most important inter- and intramolecular interactions.

1. Introduction

Ciprofloxacin (CIP), 1-cyclopropyl-6-fluoro-4-oxo-7-piperazin-1-yl-quinoline-3-carboxylic acid, is a widely prescribed, broad-spectrum oral fluoroquinolone antibiotic approved for the treatment of several types of infections (Clinical Pharmacology, 2007). It is active against both Gram negative and Gram positive bacteria (Hooper and Wolfson, 1993). In aqueous solutions CIP exists mainly in its zwitterionic form, due to the acid base interaction between the piperazine basic nitrogen and the carboxylic group. As a consequence the aqueous solubility of CIP at pHs close to 7 (isoelectric point of the molecule) is low (0.088 mg/ml) (Fallati et al., 1994; Romañuk et al., 2009). This property makes it difficult to formulate optimized liquid dosage forms such as parenteral, ototopic or ophthalmic solutions (Takács-Novák et al., 1990). Moreover, fluoroquinolones are characterized by a bitter taste (Pisal et al., 2004; Hee-Kim and Hoo-Kyun, 2004; Shirai et al., 1994), which is an additional complication for the oral administration of these compounds. Recent investigations have shown incomplete dissolution of CIP hydrochloride tablets at intestinal pH 6.8, due to its poor solubility (Breda et al., 2009). Also, it has been proposed that CIP bioavailability can be limited by both solubility and permeability (Breda et al., 2009). For active pharmaceutical ingredients (APIs) with solubility-limited bioavailability, a challenging task in the development of the product is to improve their solubility without compromising other performance. Indeed, a widely accepted approach to overcome poor solubility of an API is the preparation of their salt forms.

We have previously reported some saccharinate salts of a number of related fluoroquinolone antimicrobials (viz., ciprofloxacin, norfloxacin, enrofloxacin and ofloxacin) (Romañuk et al., 2009). Saccharin was selected as the counterion because of its sweet taste and its well known capability to form salts and cocrystals (Baran, 2005; Banerjee et al., 2005; Velaga et al., 2008). A significant improvement on aqueous solubility was observed for all the salt forms studied. In particular, for the CIP saccharin salt, (CIP-SAC) this improvement is maintained due to the ion-pair formation at pH 7 (Romañuk et al., 2009).

The aim of this work is to present a new polymorph of CIP-SAC (hereafter CIP-SAC II) and to compare it with the previously reported form CIP-SAC I (Romañuk et al., 2009). To this effect a thorough solid-state characterization of both forms have been accomplished, using techniques such as powder X-ray diffraction (PXRD), differential scanning calorimetry (DSC), thermogravimetric analysis (TGA) and infrared (IR) and solid-state nuclear

* Corresponding author. Tel.: +54 9 03514334127; fax: +54 9 03514334127.
E-mail addresses: meoliver@fcq.unc.edu.ar, miniolivera@yahoo.com.ar (M.E. Olivera).

0378-5173/$ – see front matter © 2010 Elsevier B.V. All rights reserved.
doi:10.1016/j.ijpharm.2010.03.007

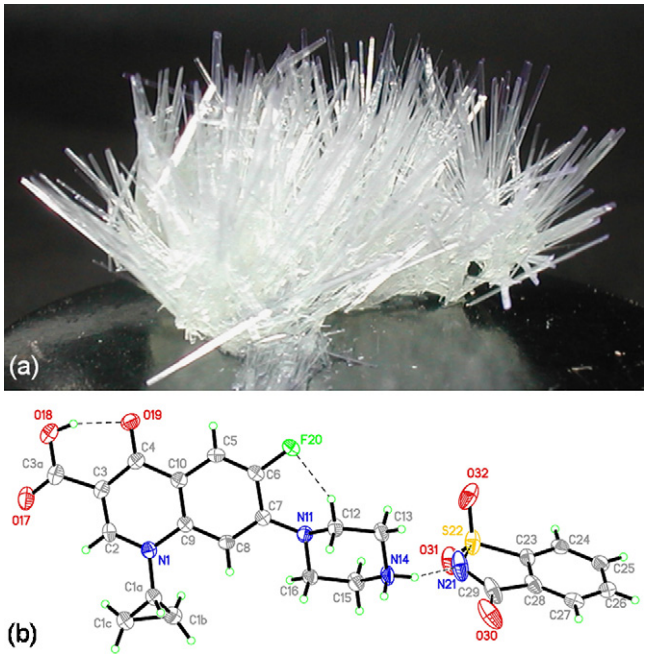

Fig. 1. (a) Single crystal of CIP-SAC II and (b) a view of CIP-SAC II asymmetric unit with some relevant intramolecular H-bonds.

magnetic resonance spectroscopy (SSNMR). The crystal structure of CIP-SAC (II) has also been determined by single crystal X-ray diffraction.

2. Experimental

2.1. Sample preparation and crystallization

CIP was obtained by neutralization of the hydrochloride salt (ciprofloxacin hydrochloride (CIP·HCl, USP, Neuland Laboratories Ltd.®), pharmaceutical grade). SAC was obtained by neutralization of the sodium salt (SAC-Na, Parafarm, China) and recrystallized from water; crystalline and anhydrous compounds were obtained and analyzed using DSC and powder X-ray diffraction techniques in order to control the reproducibility of different batches. CIP-SAC I was prepared as reported (Romañuk et al., 2009). CIP-SAC II was obtained by a slight modification of patent application P-060105581 (Manzo et al., 2009): appropriate quantities of CIP and SAC were dissolved in hot water and allowed to slowly cool in a dark place; acicular single crystals of CIP-SAC II were obtained after 2 or 3 days (Fig. 1a). These crystals were used to determine the crystal structure of the compound by X-ray diffraction and to carry on the analysis through the other techniques.

2.2. Analytical methodology

2.2.1. Single crystal and powder X-ray diffraction

Room temperature single crystal X-ray data collection was performed on a BRUKER SMART diffractometer, using SMART-NT with Bruker 2001 as the data collection driving software and SAINT-NT (Bruker, 2001) for data reduction and cell refinement. The structure was solved with SHELXS97 (Sheldrick, 2008) and refined using SHELXL97 (Sheldrick, 2008), with anisotropic displacement factors for non H atoms, and C–H hydrogen atoms stereochemically positioned, riding on their hosts. The O–H hydrogen was found in a difference map and refined with restrained O–H distance. XP in the SHELXTL-NT package was used for molecular graphics (Bruker, 2001).

Room temperature XRPD data were recorded on a RIGAKU diffractometer (Miniflex, Japon) using Cu Kα ($\lambda = 1.5417$ Å) radiation at 30 kV and 15 mA. Diffraction patterns were collected over a range of 5–50° 2θ at a scan rate of 0.01° 2θ min^{-1}.

2.2.2. Thermal analysis

The samples were subjected to differential scanning calorimetry (DSC) and thermogravimetric analysis (TGA), over a temperature range of 30–350 °C. The DSC standard cell of an A2920 MDSC (TA instruments) equipped with a data station (Universal Analysis, TA Instruments) was used to determine DSC curves. The temperature axis and the cell constant of the DSC cell were calibrated with indium (24 mg, 99.99% pure, peak maximum at 156.66 °C and heat of fusion 28.71 J/g, cell constant 1.2375). The samples (0.8–1.2 mg) were heated in crimped aluminum pans, under nitrogen flux (60 ml/min). Samples were run at 10°K/min ramps. A 2950 TGA HR thermogravimetric analyzer (TA Instruments) linked to a data station was used. The samples (0.8–1.5 mg) were placed in open aluminum pans and heated under the same conditions used in their respective DSC analysis.

2.2.3. IR and solid-state NMR spectroscopy

FT-IR spectra from 1% solid dispersions in KBr were recorded in a FT-IR Nicolet 5 SXC. High-resolution solid-state ^{13}C cross-polarization/magic angle spinning (CP/MAS) spectra for CIP-SAC I and II were recorded using a Bruker Avance II-300 spectrometer (300.13 MHz for ^{1}H and 75.46 MHz for ^{13}C). The samples were packed into a 4 mm rotor and spun with a rate of 10 kHz. The CP/MAS spectra were recorded employing a variable amplitude CP (2 ms contact time) (Harris, 1994). TPPM sequence was used for heteronuclear decoupling during acquisition with a proton field H_{1H} satisfying $\omega_{1H}/2\pi = \gamma_H H_{1H} = 60$ kHz (Bennet et al., 1995). The recycling time was 4 s. Different numbers of scans were recorded for each compound in order to obtain an adequate signal to noise ratio. The quaternary carbon edition spectra were recorded for all the samples. These spectra were acquired with the non quaternary suppression (NQS) sequence, in which the ^{1}H and ^{13}C r.f. fields are removed during 40 μs after CP and before acquisition (Harris, 1994). This experiment allowed us to identify quaternary carbon signals and methyl groups, and to perform the assignments in the solid-state. All the solid-state NMR experiments were performed at room temperature.

3. Results and discussion

3.1. X-ray diffraction techniques

Powder X-ray diffraction (PXRD) patterns of CIP-SAC polymorphs I and II presented clear differences (Fig. 2), confirming that they are different crystal forms and the technique appearing as a suitable tool for identification of both polymorphs not only during the crystallization process but also in the formulating development and manufacture.

Single crystal results: Table 1 presents some crystallographic data and refinement results for form II (CCDC, 2010), while Fig. 1b shows a view of the asymmetric unit, with the atom labelling used throughout this paper as well as the intramolecular H-bonds defining the two internal S_1^1 (6) loops hindering some torsional degrees of freedom (Bernstein et al., 1995). Bond distances and angles are normal, and the overall geometry does not deviate significantly from that on previously reported structures, as suggested by the least squares fit of the CIP unit in form II with, for instance, the one in the ciprofloxacin hexahydrate reported by Turel et al. (1997). The two molecules present a mean deviation as small as 0.21(1) Å (Fig. 3).

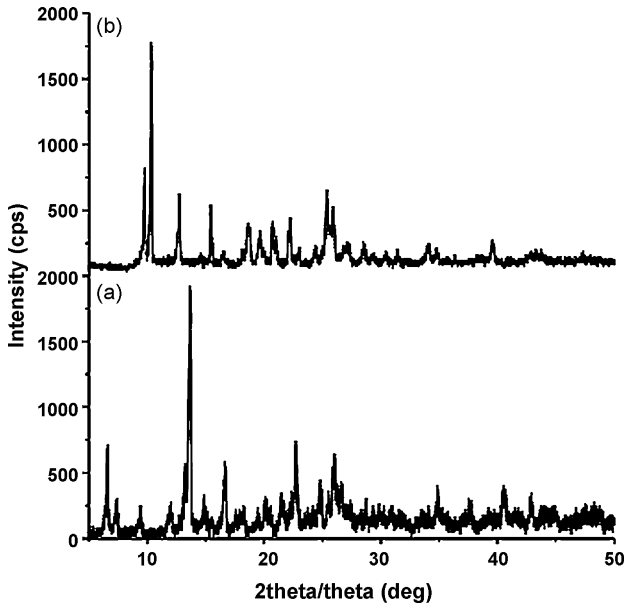

Fig. 2. PXRD patterns of CIP-SAC I powder (a) and CIP-SAC II single crystal (b).

Table 1
Crystal and refinement data for CIP-SAC II.

Empirical formula	$(C_{17}H_{19}FN_3O_3)^+ (C_7H_4NO_3S)^-$
Formula wt	514.52
Crystal system	Monoclinic
Space group	C2/c
a (Å)	37.416(2)
b (Å)	6.9051(4)
c (Å)	19.5718(12)
α (°)	90
β (°)	114.5161(10)
γ (°)	90
V (Å^3)	4600.7(5)
Z	8
ρ_{calcd} (g cm^{-3})	1.486
μ (cm^{-1})	0.199
F_{000}	2144
Index range (h,k,l)	$-48 \le h \le 47$, $-9 \le k \le 8$, $-25 \le l \le 25$
Reflections (all, unique (R_{int}), observed ($F^2 > 2\sigma(F^2)$))	18,341, 5092(0.0327), 3610
R1[a], wR2[b] ($F^2 > 2\sigma(F^2)$)	R1 = 0.0657, wR2 = 0.1679

The main differences with related CIP structures resides in the packing interactions, which in the case of CIP-SAC II are defined by conventional (O–H···O, N–H···O and N–H···N) and non-conventional (C–H···O) hydrogen bonds, as well as π–π interactions (Tables 2 and 3 and Fig. 4). The strongest of these are by far the conventional H-bonds (Four leading entries in Table 2). The first one, O18–H18···O19 is intramolecular, having the carbonyl oxygen as an acceptor and defining one of the two S_1^1 (6) cycles in the structure (the other S_1^1 (6) cycle is defined by the C12–H12B···F20 H-bond). The second, N14–H14A···N21 connects the two reference molecules into a single unit (Fig. 1b). The remaining two interactions involve the positively charged piperazinium N atom in ciprofloxacin and the oxygens of the S22=O group in the saccharine ion, to define a columnar structure built up around a family of symmetry centers at $x = 0.25$, $z = 0.25$ (in bold in Fig. 4). These columnar structures, in turn, approach each other with interleaved aromatic rings pertaining to the ciprofloxacin unit, in a typical π–π interaction defining 2D structures parallel to (0 0 1) (Table 3, see also at $x = 0, 1$; $z = 0.5$ in Fig. 4). Weaker, non-conventional C–H···O bonds connect these structures with each other along c.

Table 2
Hydrogen bonds for CIP-SAC II (Å and°).

D–H···A	d(D–H)	d(H···A)	d(D···A)	<(DHA)
O18–H18···O19	0.83(3)	1.74(3)	2.554(3)	158(4)
N14–H14A···N21	0.90	1.94	2.784(3)	155
N14–H14B···O30#1	0.90	2.26	2.974(4)	136
N14–H14B···O31#2	0.90	2.20	2.881(4)	132
C12–H12B···F20	0.97	2.24	2.890(4)	124
C1b–H1bA···O32#3	0.97	2.46	3.293(4)	144
C1b–H1bB···O19#4	0.97	2.27	3.232(4)	171
C1c–H1cB···O17#5	0.97	2.45	3.104(4)	124

Symmetry transformations used to generate equivalent atoms: #1 $-x+1/2, -y+3/2, -z+1$; #2 $x, y+1, z$; #3 $x, 1-y, 1/2+z$; #4 $-x, 1-y, 1-z$; #5 $-x, y, 3/2-z$.

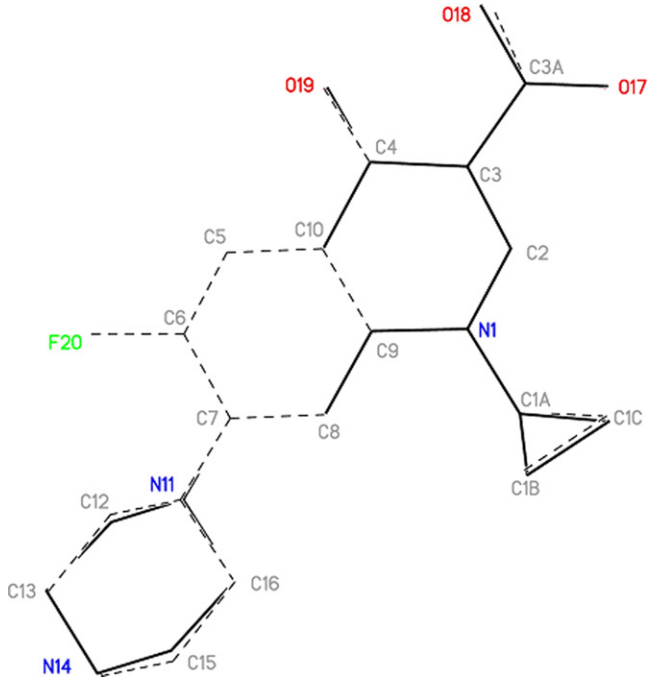

Fig. 3. Least squares fit of the ciprofloxacin unit in CIP-SAC II with the one in the ciprofloxacin hexahydrate.

Regarding the saccharinate interactions, the strong H-bond involving one oxygen in the S22=O group as an acceptor and having as a donor a protonated N group in the accompanying cation had already been reported in several other saccharinate salts (Bhatt et al., 2005). This behaviour contrasts with that of pure saccharine, in which the intermolecular interactions involving the S22=O oxygens are significantly weaker (Wardell et al., 2005). Furthermore, C29 is involved in an H-bond with one of the N14 protons as displayed in Fig. 3 while in pure saccharine this interaction is with the aromatic protons of the neighbour saccharine molecule (Wardell et al., 2005).

Table 3
π···π interactions for CIP-SAC II (Å and°).

Cg···Cg	icd (Å)	da (°)	ipd (Å)
Cg1···Cg1#1	3.7736 (14)	0.00	3.515
Cg1···Cg1#2	3.5271 (14)	0.00	3.375
Cg1···Cg2#1	3.7639 (15)	0.17	3.511
Cg1···Cg2#2	3.8210 (15)	0.17	3.379

icd: intercentroid distance, da: dihedral angle, and ipd: interplanar distance. Cg1: N1, C2, C3, C4, C10, C9; Cg2: C5, C6, C7, C8, C9, C10. #1 = $-x, 1-y, 1-z$; #2 = $-x, 2-y, 1-z$.

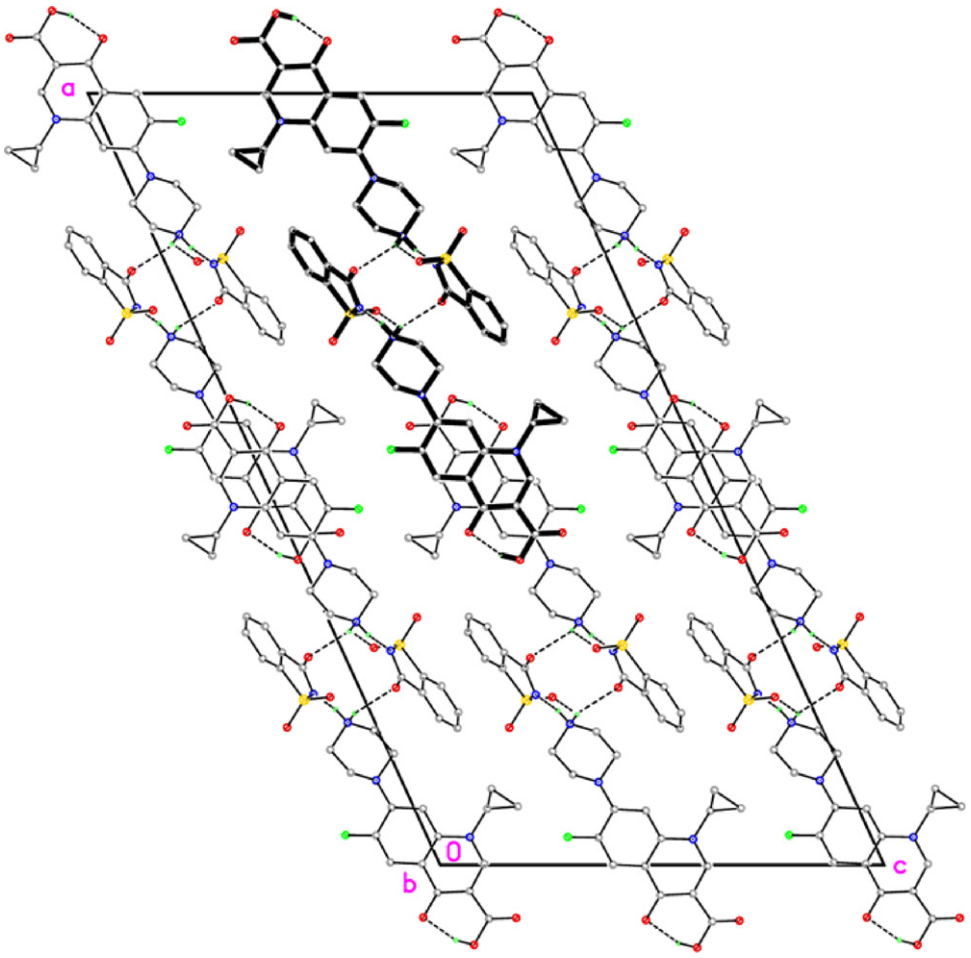

Fig. 4. A typical π–π interaction defining 2D structures parallel to (0 0 1). In bold, a columnar structure built up around a family of symmetry centers at $x = 0.25$, $z = 0.25$.

3.2. Thermal analysis

Fig. 5 shows the DSC and TGA results of CIP-SAC I and II. The DSC of CIP-SAC II exhibits one endotherm at 305.50 °C, corresponding to its melting point (onset 301.29 °C), followed by an exotherm at 310.06 °C ascribed to drug decomposition. The melting enthalpy is 372.9 J/g. CIP-SAC I shows a similar profile but with a slightly lower melting point (300.87 °C, onset 298.60 °C), and melting enthalpy 191.7 J/g. Both facts seem to suggest a weaker intermolecular linkage in I than in II, but unfortunately no single crystals of the former phase could be obtained so far so as to make a comparative structural study. In addition, no mass loss was observed in either profile when both compounds were heated from 30 °C up to fusion, indicating their anhydrous nature as well as the absence of unreacted SAC or CIP.

3.3. IR spectroscopy

Table 4 displays the FT-IR patterns of CIP-SAC I and II together with those for CIP and SAC. The characteristic absorption bands of SAC and CIP can be clearly observed. No significant differences appeared in the FT-IR patterns when both polymorphic forms were compared. In both cases, evidence of ionic interaction was obtained by following the peaks corresponding to CON(21)–H and C(29)═ONH stretching of the secondary amide at 3093 and 1725 cm^{-1}, respectively. The absence of the CON(21)–H band and the bathocromic shift of C(29)═ONH is a good insight of salt formation by proton transference from SAC amide to CIP (Fig. 6). These results are in agreement with other author's reports and are coincident with the pattern observed for these functional groups in SAC-Na (Binev et al., 1996; Yilmaz et al., 2001).

Table 4
FT-IR data for CIP-SAC I (powder), CIP-SAC II (single crystal) and their precursors CIP and SAC.

Groups	SAC	CIP	CIP-SAC I	CIP-SAC II
υ C–H olefinic and aromatics	–	3046	3027	3025
υ C3═OOH	–	np	1734	1732
υ C4═O keto	–	1627	1630	1630
υ t C29═ONH	1725	–	–	–
υ t C29═ON^-	1647[a]	–	1666	1662
υ f CON21-H	3093	–	np	np
υ_{sym} S22═O	1180	–	1148	1145
υ_{asym} S22═O	1338	–	1338	1338

np: not present.
[a] In the sodic salt.

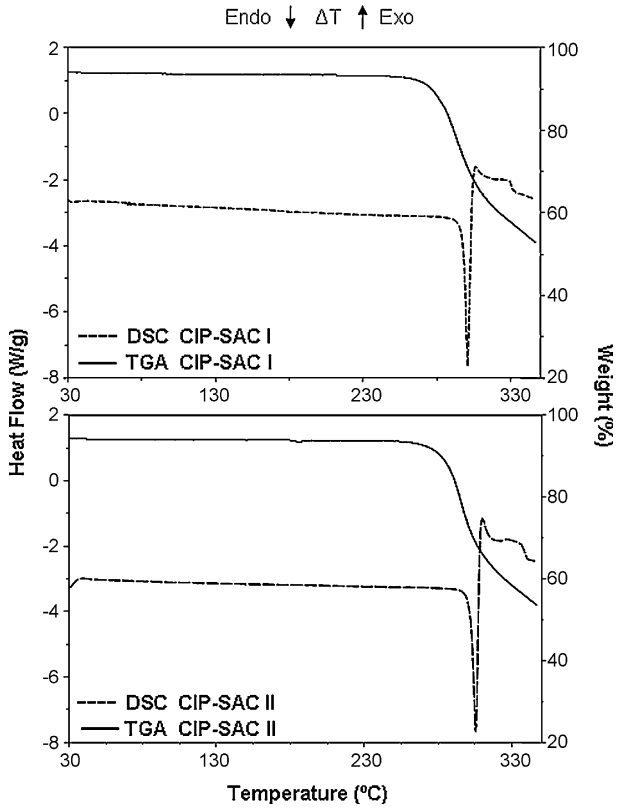

Fig. 5. Thermal analysis (DSC, TGA) curves of the homologous series of CIP-SAC I and CIP-SAC II.

As compared with free SAC, the bathocromic peak shift in the S22=O previously reported form CIP-SAC I, ascribed to hydrogen bonding interaction in the crystal structure of the salt, is also observed in CIP-SAC II.

Also, the C3a=OOH band, which is not present in CIP due to its zwitterionic nature (Romañuk et al., 2009; Turel, 2002), can be observed in CIP-SAC I and II at the same frequencies suggesting that the zwitterionic nature of CIP is reverted in both cases by proton transference from SAC.

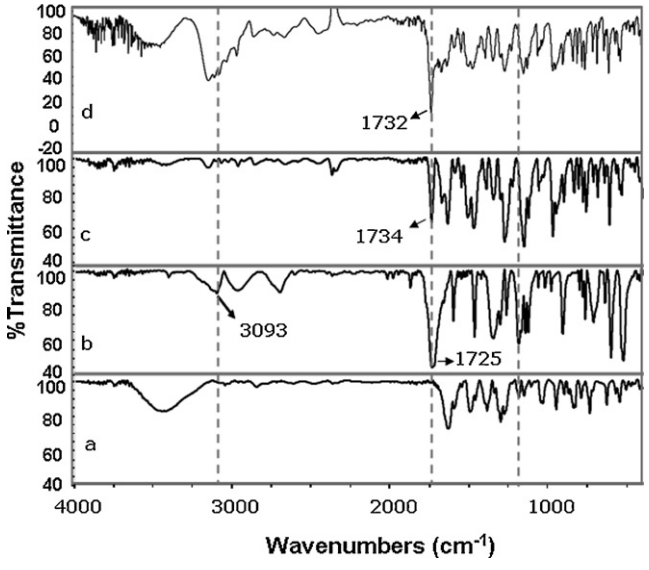

Fig. 6. The characteristic FT-IR absorption bands of CIP (a), SAC (b), CIP-SAC I (c) and CIP-SAC II (d).

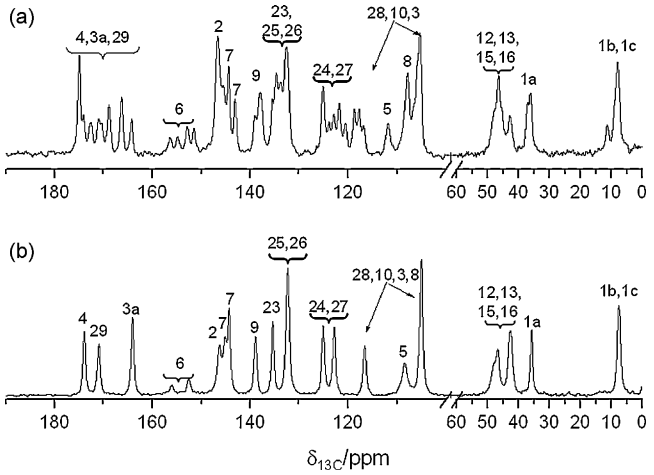

Fig. 7. ^{13}C CP/MAS spectra of: (a) CIP-SAC I and (b) CIP-SAC II.

Table 5
^{13}C chemical shifts from CP/MAS spectra of CIP-SAC I and II. The chemical shifts of the quaternary carbons are taken directly from the NQS spectra.

^{13}C	CIP-SAC I (ppm)	CIP-SAC II (ppm)
C4	174.9–174.1–172.5–170.9 170.3–168.8–166.2–164.2	173.8
C3a	Idem C4	164.0
C6	151.4–152.8–154.7–156.4	155.9–152.5
C2	146.6–145.4	146.2
C7	144.4–143.0	146.2–144.2
C9	138.0–138.9	138.8
C3, C10	116.7–105.4–117.6–118.5	116.4–104.8
C5	111.7	108.2–104.8
C8	107.6	Idem C5
C12, C13, C15, C16	46.2–42.5	46.5–42.4
C1a	35.9–36.7	35.5
C1b, C1c	11.0–7.6	7.3
C29	Idem C4	170.9
C23	134.6–132.5	135.2
C25, C26	135.3–133.7–134.6–132.5	132.2
C28	Idem C3, C10	Idem C3, C10
C24, C27	125.0–123.8–122.8–121.7–120.4	124.9–122.6

3.4. Solid-state NMR spectroscopy

The ^{13}C CP-MAS spectra of CIP-SAC I and II are shown in Fig. 7. Table 5 reports the ^{13}C chemical shifts for these samples. The NQS spectra for CIP-SAC I and II are illustrated in Fig. 8. The atomic labels correspond to Fig. 1b.

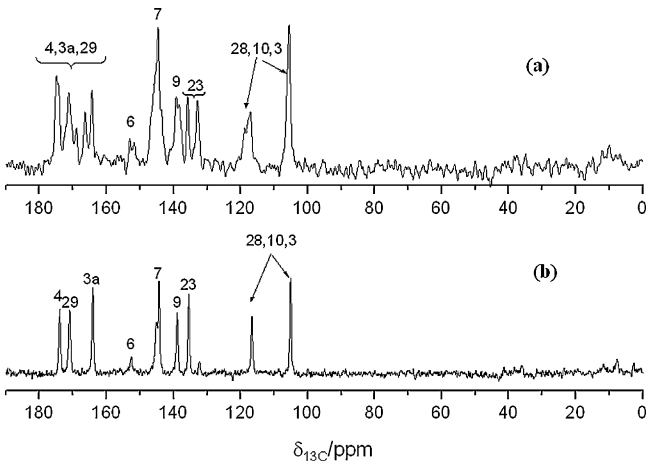

Fig. 8. NQS spectra of: (a) CIP-SAC I and (b) CIP-SAC II.

The CIP-SAC (I and II) spectra were assigned comparing with the previously reported ^{13}C CP/MAS spectra of CIP and SAC, and taking into account the NQS data of each compound (see Fig. 8) (Romañuk et al., 2009; Chattah et al., 2007).

Regarding to the CIP-SAC (I and II) spectra, they display narrow lines, giving evidence of a high degree of crystallinity and order in these compounds. These results are in agreement with our PXRD results. Besides, ^{13}C CP/MAS spectrum of CIP-SAC II confirms the observation made from crystallographic data that there is only one molecule per asymmetric unit, contrasting with the CIP-SAC I case, where there is multiplicity for the carbon resonance indicating the presence of more than one independent molecule and, therefore introducing further evidence for the existence of polymorphism in CIP-SAC.

The zwitterionic character of CIP leads to a positively charged N14. Comparing the ^{13}C SSNMR spectra of pure CIP reported in Romañuk et al. (2009) with that of the two CIP-SAC forms, no significant chemical shifts differences are observed for the carbons belonging to the piperazine group of the CIP molecule, i.e. C12, C13, C15 and C16. This is in agreement with the fact that N14 is also positively charged in CIP-SAC but due to a salt formation. It can be also noted that the resonances belonging to C4 and C3a, that in CIP appear at 173.2 ppm, splits in CIP-SACs. The position of C3a at 164.0 in CIP-SAC II points to a COOH group not negatively charged. It is also interesting to see in Fig. 8, a noticeable shift to lower ppm suffered by C3 and C10 in both polymorphs of CIP-SAC, originally at 123.3–119.8 ppm in pure CIP. Signals corresponding to C24 and C27 of the saccharine molecule appear resolved and with high intensity in CIP-SAC II. The same fact can be seen in C25 and C26. This can be due to a good crystallinity of the saccharinate. Carbonyl C29 appears at 164.0 ppm in pure SAC, then a shift to higher ppm can be clearly identified in CIP-SAC II. This shift is related to changes in the hydrogen bond involving this carbon (from homo-molecular in SAC to hetero-molecular in CIP-SAC), as predicted by XR data. C28 is difficult to assign because it appears overlapped with C10 and C3.

Finally it is interesting to note that the general features and resonance shifts observed in CIP-SAC I can also be observed in CIP-SAC II, for example the shifts in C3, C10, C28, C29. Thus NMR would indicate some degree of qualitative similarity in the intermolecular interaction scheme in both polymorphs, while thermal analysis data might indicate a difference in quantitative terms.

4. Conclusions

A new polymorph of ciprofloxacin saccharinate (CIP-SAC II) was identified and characterized by single crystal structure determination and solid-state techniques as FT-IR, DSC, TGA, ^{13}C SSNMR, PXRD. The combination of the applied techniques (FT-IR, DSC, TGA, ^{13}C SSNMR, PXRD) together with the structural data show consistent results and allows the unambiguous identification of both polymorphs. Structural analysis performed on CIP-SAC II single crystals shows the compound to be a stable anhydrous salt with typical inter- and intramolecular interactions.

From PXRD analysis it can be concluded that both polymorphs are crystalline solids, also confirmed by ^{13}C CP/MAS NMR spectra. Thermal analysis gives evidence about the absence of unreacted SAC as well as the anhydrous nature of the compounds. In both saccharinates, evidence of ionic interaction was obtained by FT-IR giving a good insight of salt formation by proton transference from SAC amide to the FQ. The zwitterionic character of CIP is reverted by salt formation in CIP-SAC I and II. This effect can be concluding from the FT-IR spectra of both polymorphs, and also from ^{13}C CP/MAS. Changes in H-bond nature, from homo-molecular in SAC to hetero-molecular in CIP-SACs, are clearly identified by FT-IR and ^{13}C CP/MAS, confirming the predictions done by XR.

The similarity of some general features, FT-IR and ^{13}C resonance shifts observed in both ^{13}C SSNMR spectra suggests that the interaction scheme found for CIP-SAC II could be applicable to CIP-SAC I as well.

Acknowledgements

This work was partially supported by CONICET, SeCyT-UNC, MinCyT Córdoba, ANPCyT-FONCyT. Dra. Cuffini thanks Fundación Sauberan.

References

Banerjee, R., Bhatt, P.M., Ravindra, N.V., Desiraju, G.R., 2005. Saccharin salts of active pharmaceutical ingredients, their crystal structures, and increased water solubilities. Cryst. Growth Des. 5, 2299.

Baran, E.J., 2005. The saccharinate anion: a versatile and fascinating ligand in coordination chemistry. Quim. Nova 28, 326.

Bennet, A.E., Rienstra, C.M., Auger, M., Lakshmi, K.V., Griffin, R.G.J., 1995. Heteronuclear decoupling in rotating solids. Chem. Phys. 103, 6951.

Bernstein, J., Davis, R.E., Shimoni, L., Chang, N.L., 1995. Patterns in hydrogen bonding: functionality and graph set analysis in crystals. Angew. Chem. Int. Ed. Engl. 34, 1555.

Bhatt, P.M., Ravindra, N.V., Banerjee, R., Desiraju, G.R., 2005. Saccharin salts of active pharmaceutical ingredients, their crystal structures, and increased water solubilities. Chem. Commun. 28, 1073.

Binev, I.G., Stamboliyska, B.A., Velcheva, E.A., 1996. The infrared spectra and structure of o-sulfobenzimide (saccharin) and of its nitranion: an ab initio force field treatment. Spectrochim. Acta A 52, 1135.

Breda, S.A., Jimenez Kairuz, A.F., Manzo, R.H., Olivera, M.E., 2009. Solubility behavior and biopharmaceutical classification of novel high-solubility ciprofloxacin and norfloxacin pharmaceutical derivatives. Int. J. Pharm. 371, 106.

CCDC 737186 contains the supplementary crystallographic data for this paper. These data can be obtained free of charge from The Cambridge Crystallographic Data Centre via www.ccdc.cam.ac.uk/data_request/cif.

Chattah, A.K., Garro Linck, Y., Monti, G.A., Levstein, P.R., Breda, S.A., Manzo, R.H., Olivera, M.E., 2007. NMR and IR characterization of the aluminium complexes of norfloxacin and ciprofloxacin fluoroquinolones. Magn. Reson. Chem. 45, 850–859.

Clinical Pharmacology, 2007. Ciprofloxacin [Internet, Restricted Access]. Clinical Pharmacology A Gold Standard Product An Elsevier Company (cited 2009 July 10). Available from: http://clinicalpharmacology.com/Forms/drugoptions.aspx?cpnum=127&n=Ciprofloxacin.

Fallati, C.S., Ahumada, A.A., Manzo, R.H., 1994. El Perfil de Solubilidad de la Ciprofloxacina en Función del pH. Acta Farmacéut. Bonaerense 13, 73.

Harris, R.K., 1994. Nuclear Magnetic Resonance Spectroscopy. Longman Scientific and Technical, London, UK.

Hee-Kim, E., Hoo-Kyun, C., 2004. Preparation of various solid-lipid beads for drug delivery of enrofloxacin. Drug Deliv. 11, 365.

Hooper, D.C., Wolfson, J.S., 1993. Quinolone Antimicrobial Agents, 2nd ed. American Society for Microbiology.

Manzo, R.H., Olivera, M.E., Romañuk, C.B., Universidad Nacional de Córdoba, 2009. Procedimiento para Obtención de Sacarinatos de Antimicrobianos Fluoroquinolónicos y los Sacarinatos Obtenidos. Córdoba, Argentina. Solicitud de patente P-060105581, 18/12/06. Publicada 11/02/09, Boletín N° 516, p. 4. ISS N 0325-6545. Instituto Nacional de la Propiedad Industrial.

Pisal, S., Zainnuddin, R., Nalawade, P., Mahadik, K., Kadam, S., 2004. Molecular properties of ciprofloxacin-indion 234 complexes. AAPS Pharm. Sci. Technol. 22 5, 1.

Romañuk, C.B., Garro Linck, Y., Chattah, A.K., Monti, G.A., Manzo, R.H., Olivera, M.E., 2009. Characterization of the solubility and solid-state properties of saccharin salts of fluoroquinolones. J. Pharm. Sci. 98, 3788.

Shirai, Y., Sogo, K., Fujioka, H., Nakamura, Y., 1994. Role of low-substituted hydroxypropylcellulose in dissolution and bioavailability of novel fine granule system for masking bitter taste. Biol. Pharmaceut. Bull. 17, 427.

Takács-Novák, K., Noszal, B., Hermecz, I., Kereszturi, G., Podanyi, B., Szasz, G., 1990. Protonation equilibria of quinolone antibacterials. J. Pharm. Sci. 79, 1023.

Turel, I., 2002. The interactions of metal ions with quinolone antibacterial agents. Coord. Chem. Rev. 232, 27.

Turel, I., Bukovec, P., Quirós, M., 1997. Crystal structure of ciprofloxacin hexahydrate and its characterization. Int. J. Pharm. 152, 59.

Velaga, S.P., Basavoju, S., Boström, D., 2008. Norfloxacin saccharinate–saccharin dihydrate cocrystal—a new pharmaceutical cocrystal with an organic counter ion. J. Mol. Struct. 889, 150.

Wardell, J.L., Low, J.N., Guidewell, C., 2005. Saccharin, redetermined at 120 K: a three-dimensional hydrogen-bonded framework. Acta Cryst. E61, 1944–1946.

Yilmaz, V.T., Topcu, Y., Yilmaz, F., Thoene, C., 2001. Saccharin complexes of Co(II), Ni(II), Cu(II), Zn(II), Cd(II) and Hg(II) with ethanolamine and diethanolamine: synthesis, spectroscopic and thermal characteristics. Crystal structures of $[Zn(ea)_2(sac)_2]$ and $[Cu_2(\mu\text{-dea})_2(sac)_2]$. Polyhedron 20, 3209.